OXFORD

The Rejuvenation and Functional Restoration of Aged Adipose Stem Cells by DUXAP10 Knockdown via the Regulation of the miR-214-3p/RASSF5 Axis

Sen Ren[1,‡], Chengcheng Li[2,‡], Hewei Xiong[3,‡], Qian Wu[1], Xiaohui Wu[1], Zhongwei Xiong[1], Lixing Dong[1,4], Bing Shu[1], Wei Wei[1], Chao Ma[1,*], Xiang Li[1,4,5,*], Jincao Chen[1,*]

[1]Department of Neurosurgery, Zhongnan Hospital of Wuhan University, Wuhan, People's Republic of China
[2]Department of Hand Surgery, Union Hospital, Tongji Medical College, Huazhong University of Science and Technology, Wuhan, People's Republic of China
[3]Department of Emergency Surgery, Union Hospital, Tongji Medical College, Huazhong University of Science and Technology, Wuhan, People's Republic of China
[4]Brain Research Center, Zhongnan Hospital of Wuhan University, Wuhan, People's Republic of China
[5]Medical Research Institute, Wuhan University, Wuhan, People's Republic of China

*Corresponding author: Jincao Chen, Department of Neurosurgery, Zhongnan Hospital of Wuhan University, Wuhan 430071, People's Republic of China. Email: chenjc2020@126.com; or, Xiang Li, Department of Neurosurgery, Zhongnan Hospital of Wuhan University, Wuhan 430071, People's Republic of China. Email: li.xiang@whu.edu.cn; or, Chao Ma, Department of Neurosurgery, Zhongnan Hospital of Wuhan University, Wuhan 430071, People's Republic of China. Email: mcwtt318310@hotmail.com
‡Contributed equally to this work.

Abstract

Adipose stem cell (ASC)-based therapies provide an encouraging option for tissue repair and regeneration. However, the function of these cells declines with aging, which limits their clinical transformation. Recent studies have outlined the involvement of long non-coding RNAs in stem cell aging. Here, we reanalyzed our published RNA sequencing (RNA-seq) data profiling differences between ASCs from young and old donors and identified a lncRNA named double homeobox A pseudogene 10 (DUXAP10) as significantly accumulated in aged ASCs. Knocking down DUXAP10 promoted stem cell proliferation and migration and halted cell senescence and the secretion of proinflammatory cytokines. In addition, DUXAP10 was located in the cytoplasm and functioned as a decoy for miR-214-3p. miR-214-3p was downregulated in aged ASCs, and its overexpression rejuvenated aged ASCs and reversed the harm caused by DUXAP10. Furthermore, Ras Association Domain Family Member 5 (RASSF5) was the target of miR-214-3p and was upregulated in aged ASCs. Overexpressing DUXAP10 and inhibiting miR-214-3p both enhanced RASSF5 content in ASCs, while DUXAP10 knockdown promoted the therapeutic ability of aged ASCs for skin wound healing. Overall, this study offers new insights into the mechanism of age-related ASC dysfunction and names DUXAP10 and miR-214-3p as potential targets for energizing aged stem cells.

Key words: adipose stem cell; aging; non-coding RNA; DUXAP10; miR-214-3p; RASSF5.

Graphical Abstract
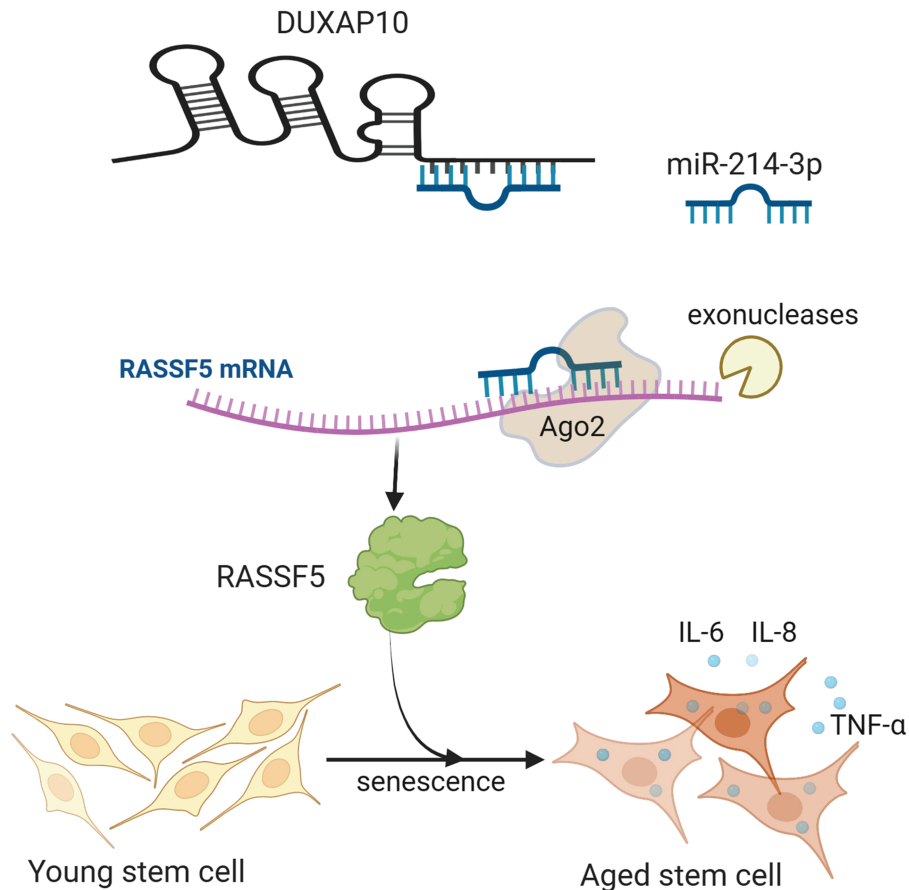
Introduction

Stem cells play a vital role in tissue homeostasis and regeneration. However, the life-long residence of stem cells in the tissue niche makes them susceptible to the accumulation of cellular damage, which would result in stem cell senescence, exhaustion, and dysfunction.[1] These age-associated detrimental changes ultimately lead to retarded reactions to cellular injury and an inferior effectiveness in tissue restoration, both of which are crucial to the causation of age-related diseases.[2] Mesenchymal stem cells (MSCs), which can be isolated from bone marrow, adipose tissue, umbilical cord, peripheral blood, urine, and so on, have seen wide studies and an extensive application in the field of translational medicine. Their functions also decline with age, which hinders their clinical application.

As vital members of MSCs, adipose stem cells (ASCs) exhibit favorable features of easy isolation and amplification, low immunogenicity, and extensive immunomodulatory effects.[3] In the past few decades, ASCs have been recognized as a promising tool for cell-based therapy and have been shown to possess beneficial effects in treating various human diseases, including skin wound healing, nerve injury, cardiac injury, immune disorders, stroke, and other ischemic diseases.[4-6] However, ASCs isolated from the elderly are demonstrably limited in their ability to repair tissues.[7] These ASCs from elderly bodies exhibit reduced proliferative and migrative capabilities, decreased multilineage differentiation potential, increased senescent features, and a proinflammatory secretome.[8-11] Thus, understanding the

underlying mechanisms of age-related ASC aberration could yield an opportunity to restore their regenerative potential.

The molecular processes involved in age-related stem cell dysfunction are rather complicated and multifactorial, including toxic metabolite accumulation, proteostasis disruption, mitochondrial and ribosomal dysfunction, endoplasmic reticulum (ER) stress, DNA damage, and epigenetic alterations.[12] According to past studies, aged ASCs present with increased intracellular reactive oxygen species (ROS) and ER stresses.[9] 5-Hydroxymethylcytosine (5hmC), an intermediate metabolite of DNA demethylation, accumulates in aged ASCs, pointing to a possible epigenetic drift in age-dependent deterioration.[13] Moreover, the efficiency of base excision repair (BER) is impaired in aged ASCs, resulting in the age-associated decline in genome integrity.[14] Still, the specific drivers and effectors responsible for ASC dysfunction in the elderly remain to be fully elucidated.

Long non-coding RNAs (lncRNAs) are defined as clusters of transcripts lengthier than 200 nucleotides, which can function as transcriptional regulators, epigenetic modifiers, molecular scaffolds of RNA and proteins, and encode small peptides.[15] Increasing evidence indicates that lncRNAs play a vital role in cellular senescence and stem cell fate determination.[16] In one recent investigation, lncRNA LYPLAL1 antisense RNA1 was downregulated significantly in senescent ASCs, but the overexpression of this lncRNA reversed the senescence phase by inhibiting MIRLET7B transcription.[17] Li et al found lncRNA Bmncr to rejuvenate aged bone marrow mesenchymal stem cells (BMSCs) and

promote their capacity for bone formation by activating the BMP2 pathway.[18] Our previous study using transcriptome profiling identified numbers of differentially expressed lncRNAs in aged ASCs.[8] However, the distinct functions of these lncRNAs in the age-related damage of ASCs are still to be disclosed.

In the present study, we reanalyzed our previous RNA-seq data comparing young ASCs to old ASCs and found a double homeobox A pseudogene 10 (DUXAP10) that accumulated significantly in old ASCs. LncRNA DUXAP10, a member of the DUXA homeobox gene family, functions as a promising oncogene promoting cancer cell proliferation and invasion.[19] Conversely, we established DUXAP10 as a negative regulator of ASC proliferation and migration and a driver of ASC senescence, which was potentially mediated through miR-214-3p sponging to enhance Ras association domain family member 5 (RASSF5) expression. Knocking down DUXAP10 rejuvenated old ASCs and promoted their ability to repair wounds. Thus, our findings postulate a new mechanism underlying age-related ASC dysfunction and provide novel targets for the restoration of the therapeutic potential of aged stem cells.

Materials and Methods

Cell Isolation and Culture

Fresh subcutaneous adipose tissue was rinsed with Dulbecco's modified Eagle's medium (DMEM, Gibco) supplemented with 1% penicillin/streptomycin to eliminate blood cells. Subsequently, the tissue was mechanically minced and subjected to digestion with 0.2% collagenase type I (Sigma) at 37 °C for 1.5 hours. The digested tissue underwent centrifugation at 300 g for 10 minutes, and the resulting cell pellets were resuspended and filtered through a 70-µm filter (Corning). The cells were then centrifuged at 300 g for 5 minutes and resuspended in a culture medium comprising DMEM supplemented with 10% fetal bovine serum (Oricell). The cells were incubated in a 37 °C incubator with 5% CO_2, and the culture medium was replenished every 3 days until reaching 80% confluence. Passage of the cells was carried out using 0.25% trypsin (Gibco), and the cells were cryopreserved in a liquid nitrogen container. The pertinent characteristics of the ASCs' donors are detailed in Supplementary Table S1. Human foreskin fibroblasts were cultured in DMEM/F12 supplemented with 10% FBS (Serapro). For all experiments, cultured ASCs and fibroblasts were used between passages 3 and 7.

Cell Proliferation, Migration, and Senescence

ASCs from various groups were seeded in 96-well culture plates (2000 cells per well). After 2 days of incubation, the proliferation rate in each group was assessed with a EdU Kit according to the manufacturer's instructions (Ribobio). ASCs suspended in DMEM (20 000 cells per well) were seeded in the upper compartment of the 24-well Transwell Chamber (8.0 µm pore size, Boster), and then incubated in complete culture media. Next day, the migrated ASCs were stained and counted under the microscope. ASCs from various groups were seeded in 48-well culture plates (5000 cells per well). After 2 days of incubation, the senescent ASCs were stained using the β-gal Staining kit (#9860, CST) according to the manufacturer's instructions.

Wound Scratch

ASCs from various groups were seeded in 6-well culture plates (100 000 cells per well). After 3 days of incubation, the complete culture media were replaced with DMEM without FBS and remained for 24 hours. The ASC supernatants were then collected as conditional media and stored at –80 °C. For wound scratch, fibroblasts were seeded in 12-well culture plates until 100% confluent, and then scored with a 200-µL pipette tip. Next, fibroblasts were incubated in the different conditional media for 2 days and then stained with the Crystal Violet.

5′ and 3′ RACE Assay

The 5′ and 3′ RACE assay was performed to identify the full length of DUXAP10 using the SMARTer RACE cDNA amplification kit (Takara) according to the manufacturer's instructions. The specific primers used for the RACE assay are described in Supplementary Table S2.

RT-PCR

Total RNAs were isolated using the miRNeasy Mini Kit (Qiagen, Germany). miRNAs were transcribed into cDNAs using the Mir-X miRNA First Strand Synthesis kit (#RR638315, TaKaRa), while mRNAs and lncRNAs were transcribed into cDNAs using the HiScript II RT kit (Vazyme, Nanjing, China). Real-time PCR was detected under the StepOnePlus platform (Applied Biosystems) using the HiScript II One Step RT-PCR SYBR Green Kit (Vazyme). The relative expression levels of the targeted genes were normalized to β-actin, GAPDH, and U6, and then calculated using the $2^{-\Delta\Delta Ct}$ method. The cytoplasmic and nuclear RNAs were isolated using the Cytoplasmic & Nuclear RNA Purification Kit (Norgen Biotek Corp). The RNAs were then transcribed into cDNAs and detected using the above methods. GADPH and U3 were used as cytoplasm-located and nucleus-located markers separately. The primers used in the PCR were described in Supplementary Tables S3 and S4.

Western Blot

We performed a Western blot using our previously established procedures.[4] A total of 30 µg of protein was separated using SDS-PAGE (Beyotime Biotechnology), transferred to a PVDF membrane, blocked for 1 hour, and then incubated with primary antibodies overnight at 4 °C. The following day, the membranes were washed 3 times, incubated with appropriate secondary antibodies (Aspen) for 1 hour, and then exposed using X-ray film (UVP). The primary antibodies used were GAPDH (#10494-1-AP, Proteintech), fibronectin 1 (#15613-1-AP, Proteintech), p21 (#10355-1-AP, Proteintech), and RASSF5 (Santa Cruz Biotechnology).

Bioinformatics Analysis

The RNA-seq data used in this study were obtained from a previously published article and had been deposited in the Gene Expression Omnibus (http://www.ncbi.nlm.nih.gov/geo; GSE174502). The analysis of differential expression for miRNAs, mRNAs, and lncRNAs was conducted using DEGseq, with fold changes defined as ≥2 or ≤–2 and *q* value < 0.001. The potential miRNAs targeted by DUXAP10 and the genes targeted by miR-214-3p were examined using 3 databases (RNAhybrid [https://bibiserv.cebitec.uni-bielefeld.de/rnahybrid], miRanda [http://www.microrna.org/], and

TargetScan [http://www.targetscan.org]). The biological functions of the targeted genes were determined using the GO database (http://geneontology.org).

Luciferase Reporter Assay

The wild and mutant types of RASSF5 3′UTR and DUXAP10 were constructed and inserted into the psiCHECK2 luciferase reporter vector (Promega). HEK-293T cells were transfected with the above vectors and miR-214-3p mimic or mimic-NC at the same time by using the Lipofectamine 2000 (Invitrogen). After a 2-day incubation period, renilla and firefly luciferase activities of these transfected cells were detected using the Dual-Luciferase Reporter Assay System Kit (E1910, Promega).

Oligonucleotide Transfection

The miR-214-3p mimic, antagomir, and negative controls were purchased from RiboBio (Guangdong). The sequences of these oligonucleotides are listed in Supplementary Table S5. Transfection was performed using the riboFECT CP Reagent (RiboBio) according to the manufacturer's protocols.

Lentiviral Vectors Construction and Stable Transfection

The entire sequence of DUXAP10, and its small hairpin RNAs of DUXAP10 was synthesized and cloned into the pLenti-EF1a-mCherry-P2A-puro-CMV and pLKD-CMV-mCherry-puro-U6-shRNA vectors (OBiO) separately. Next, the lentiviral vectors were packaged in OBiO Technology. The small hairpin RNA of RAASF5 were synthesized and purchased from HanBio. ASCs were seeded in 6-well culture plates until reaching 40% confluent, and then transfected with the aforementioned vectors following the manufacturer's instructions. The siRNA sequences for DUXAP10 and RASSF5 are listed in Supplementary Table S6.

Wound Healing Model

All animal experiments were conducted in accordance with the protocols approved by the Animal Care Committee of Tongji Medical College. Adult male Sprague-Dawley rats, aged 10 weeks, were housed at room temperature with a consistent 12-hour light/dark cycle, with up to 4 animals per cage and access to food and water ad libitum. The rats were then randomly assigned to 1 of 4 groups ($n = 5$): sh-DUXAP10 O-ASC, sh-NC O-ASC, sh-NC Y-ASC, and PBS. Following general anesthesia induced by intraperitoneal injections of xylazine (0.25 mg/kg) and ketamine (0.025 mg/kg), a full-thickness cutaneous wound (18 mm diameter) was excised on the rats' backs, and then subcutaneously injected with the aforementioned ASCs (1 000 000 per rat) or an equal volume of PBS around the wound area. All wounds were covered with an adhesive wound dressing (FB0607C, Jiangxi 3L Medical Products Group), which was changed every 3 days. Photographs of the skin wounds were taken on days 1, 4, 8, 12, and 15, and the wound size was calculated using ImageJ software.

Histological Analysis

The wound samples were harvested and embedded on day 15 after the rats euthanization. Then the wound sections were stained with H&E and masson staining kits to evaluate wound beds and collagen accumulation. The embedded wound sections were deparaffinized and incubated with the anti -PCNA antibody (Abcam, 1:200) overnight at 4 °C, and then incubated with an HRP-conjugated secondary antibody (Aspen, 1:400) for 1 hour at room temperature. The wound samples stored at –80 °C were initially embedded with OCT and sliced into a 4-μm-thick section, then incubated with an anti-α-smooth muscle actin (α-SMA) antibody (Abcam, 1:200) at 4 °C overnight, and subsequently incubated with an Alexa488-conjugated secondary antibody (Invitrogen, 1:400) for 1 hour at room temperature, and finally stained with the 4′,6-diamidino2-phenylindole (DAPI, Sigma-Aldrich).

Statistics

All data were analyzed using Graph Pad prism v 7.0 software and presented as the mean ± SEM. Statistical analysis was conducted using unpaired Student's *t* test for 2 groups and 1-way or 2-way ANOVA with Bonferroni post hoc test for more than 2 groups. The correlation between 2 RNAs' levels was evaluated using Pearson correlation coefficients. Statistical significance was considered at $P < .05$.

Results

DUXAP10 is a Candidate Pseudogene Upregulated in O-ASC

Using RNA-seq previously, hundreds of differentially expressed noncoding transcripts were found in ASCs from old and young donors.[8] In the current study, the top 10 lncRNAs were selected based on their expression levels, fold change, and *P* value, as illustrated in a hierarchical clustering heat map (Fig. 1A). Further PCR analyses revealed that DUXAP10 and DUXAP9 were significantly upregulated in O-ASC (Fig. 1B). Because DUXAP10 and DUXAP9 are double homeobox A pseudogenes with lots of similar sequences (Fig. 1C), one of the 2, in this case, DUXAP10, was selected for subsequent scrutiny, since it was far more abundant in ASC than DUXAP9. 5′-RACE (Fig. 1D-1E) and 3′-RACE (Fig. 1F, 1G) assays were conducted to ascertain the full sequences of DUXAP10. Per results from Sanger sequencing, the total length of DUXAP10 was 2398 nucleotides and a poly(A) tail (Fig. 1H), which was consistent with the sequence in GenBank.

Knocking Down DUXAP10 Promotes O-ASC Migration and Proliferation and Delays Cell Senescence

To further validate the result above, the sample volume was increased for experimentation, and more compelling evidence was obtained, as shown in Fig. 2A. To affirm this pseudogene's function, lentivirus vectors were constructed to overexpress or knockdown DUXAP10 in ASCs. The efficiency of these vectors was assessed using the PCR analysis, as shown in Fig. 2B, 2C. knocking down DUXAP10 significantly promoted O-ASC proliferation and migration in EdU (Fig. 2D, 2E and Supplementary Fig. S1A, S1B) and transwell (Fig. 2F, 2G and Supplementary Fig. S1C, S1D) migration assays. On the other hand, overexpressing DUXAP10 in Y-ASC reduced cellular proliferation and migration. According to the SA-β-gal staining assay, knocking down DUXAP10 markedly decreased the proportion of senescent cells in O-ASC, while DUXAP10 overexpression increased senescent cell numbers in Y-ASC (Fig. 2H, 2I and Supplementary Fig. S1E, S1F). Conditional media isolated from DUXAP10-overexpressed Y-ASC

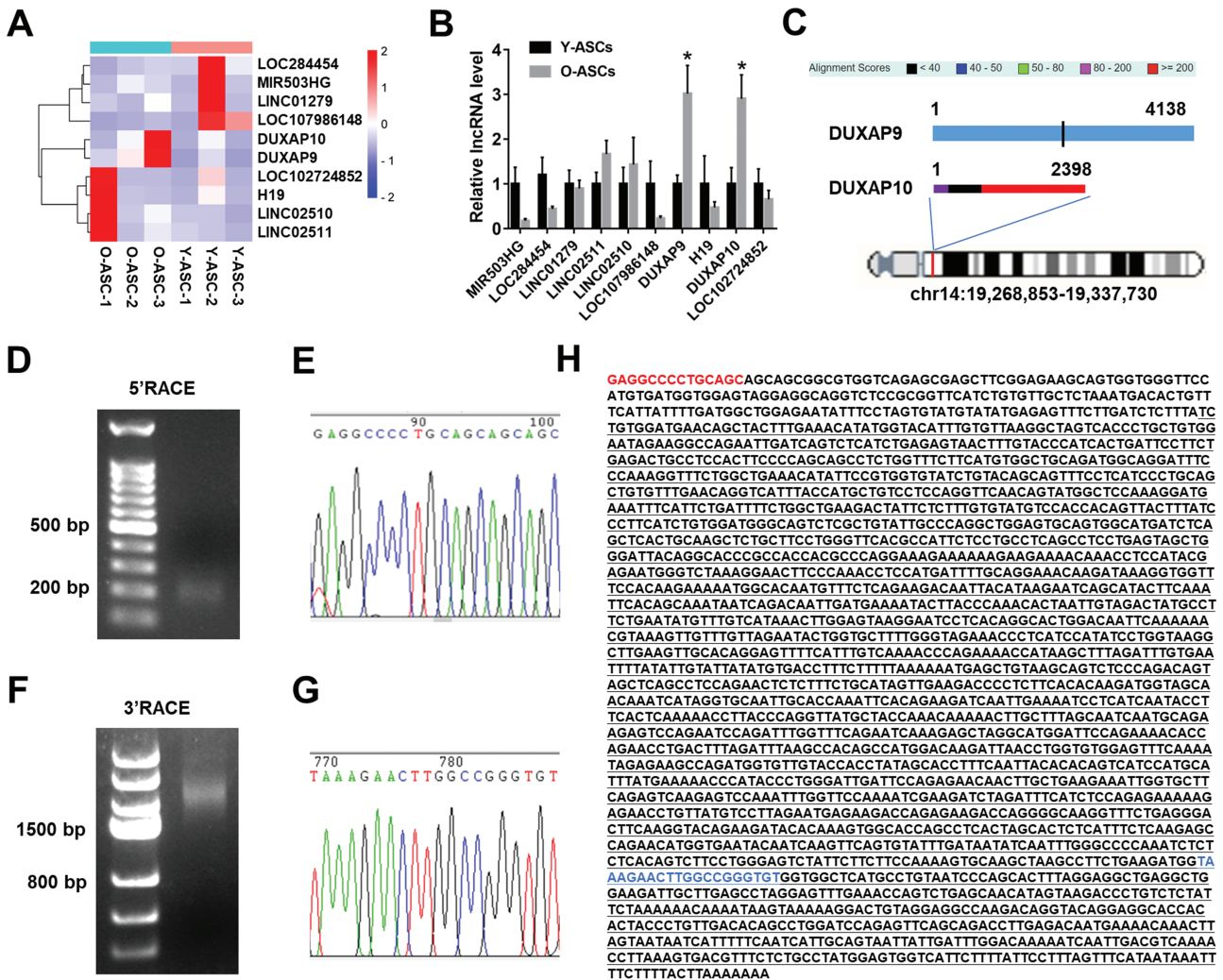**Figure 1.** Identification of a candidate lncRNA DUXAP10 in ASCs during aging. (**A**) Heatmap exhibiting the top 10 dysregulated lncRNAs between O-ASC and Y-ASC. (**B**) PCR validation of the levels of those lncRNAs; $n = 5$. (**C**) Location of DUXAP10 on chromosome 14 and comparison of the RNA sequences between DUXAP9 and DUXAP10. (**D**) RNA gel blot of the 5′RACE result. (**E**) The partial data of the Sanger sequencing on the 5′RACE result. (**F**) RNA gel blot of the 3′RACE result. (**G**) The partial data of the Sanger sequencing on the 3′RACE result. (**H**) The full length of DUXAP10 obtained from the 5′RACE (non-underlined sequences) and 3′RACE (underlined sequences) analyses. *$P < .05$, **$P < .01$, ***$P < .001$.

exhibited an inferior capacity to promote fibroblast migration compared to the negative control, whereas the knockdown of DXUAP10 enhanced this capacity in aged ASCs (Fig. 2J, 2K). Results from the Western blot assay demonstrated that knocking down DUXAP10 increased the degree of expression of migration-associated protein fibronectin 1 (FN1) and decreased the expression levels of senescence-associated protein p21; in contrast, overexpressing DUXAP10 yielded the opposite results (Fig. 2L, 2M). Findings from PCR analyses revealed that DUXAP10 overexpression promoted the secretion of senescence-associated factors, such as IL-6, IL-8, and TNF-α, while DUXAP10 knockdown inhibited IL-8 and TNF-α secretion (Fig. 2N).

DUXAP10 Functions as a Sponge for miR-214-3p

To explore the underlying mechanism of DUXAP10 in regulating ASC function, the sub-cellular location of DUXAP10 was probed first. Using the PCR analysis, a majority of DUXAP10 transcripts were found in the cytoplasm of ASC (Fig. 3A). In a previous study, cytoplasmic lncRNAs acted as competing endogenous RNAs for sponging

miRNAs.[20] The potential of miRNAs binding with DUXAP10 was predicted utilizing RNAhybrid, miRanda, and TargetScan databases. Our previous small RNA-seq study found many upregulated miRNAs in Y-ASC compared to O-ASC. Combining these results, 5 candidate miRNAs were obtained (illustrated on the heat map in Fig. 3B). Further PCR analyses found miR-214-3p to be the only one to be upregulated significantly in Y-ASC, with the difference in expression levels between the other 4 miRNAs (miR-210-5p, miR-378a-5p, miR-370-3p, and miR-296-5p) in Y-ASC and O-ASC being insignificant (Fig. 3C). A more statistically considerable result was obtained by enlarging the sample volume (Fig. 3D). Meanwhile, the levels of DUXAP10 correlated negatively with those of miR-214-3p (Fig. 3E). The transfection of an miR-214-3p mimic attenuated DUXAP10 level in ASC (Fig. 3F). However, the overexpression of DUXAP10 had no impact on miR-214-3p level in ASC (data not shown). A dual-luciferase reporter assay was deployed to verify that there was a direct binding between miR-214-3p and DUXAP10-WT; a mutation in the seeding sequences in DUXAP10 completely abolished their ability to interact (Fig. 3G, 3H).
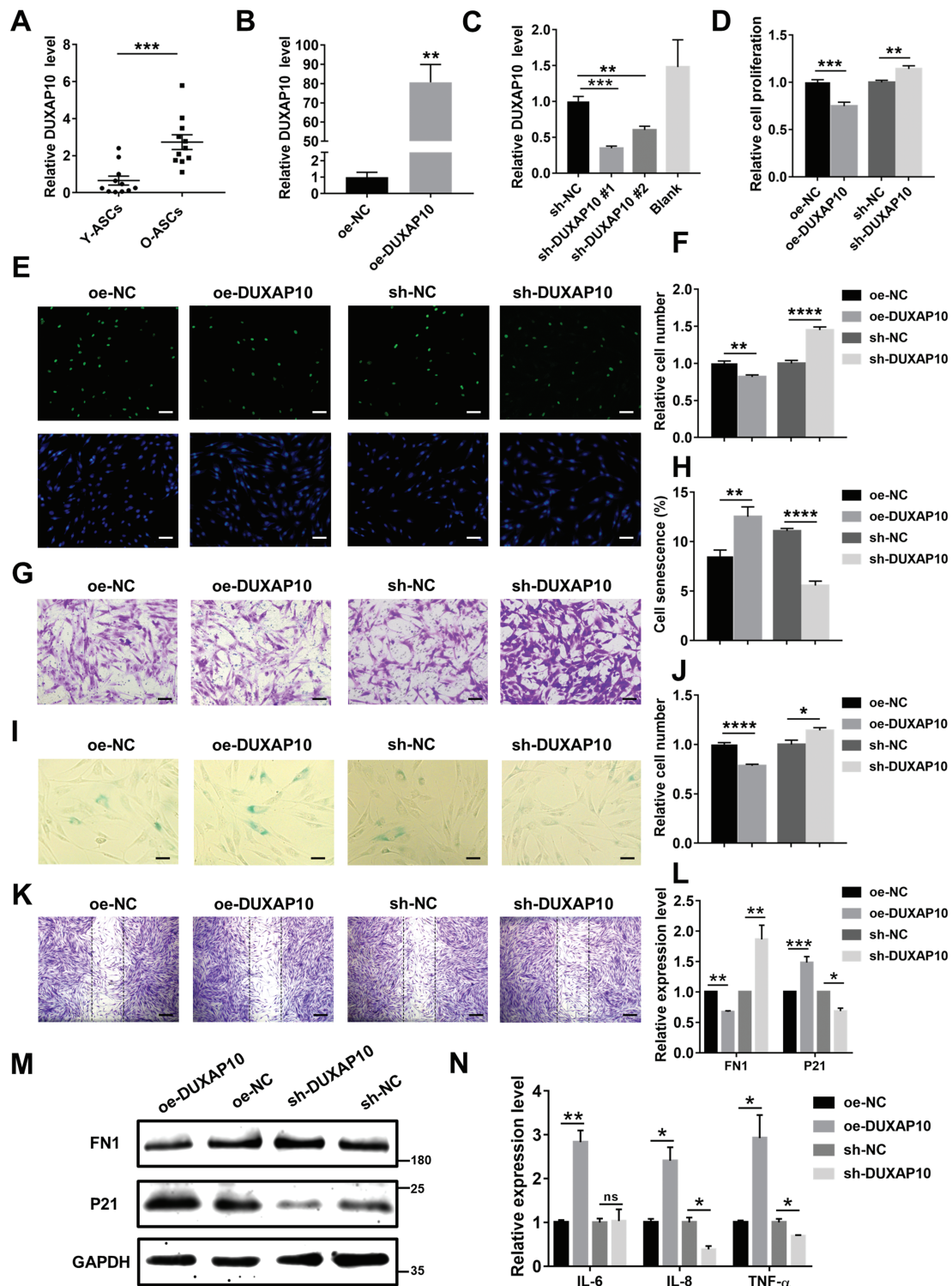
Figure 2. Knocking down DUXAP10 rejuvenated aged ASCs, while DUXAP10 overexpression impaired young ASCs. (**A**) PCR validation of the level of DUXAP10 between O-ASC and Y-ASC; $n = 11$. (**B**) PCR validation of the efficiency of the DUXAP10 overexpressed lentiviral vector. (**C**) PCR validation of the knockdown efficiency of sh-DUXAP10 lentiviral vectors. Young ASCs were transfected with a lentiviral vector overexpressing DUXAP10 (oe-DUXAP10) or a control vector (oe-NC), while aged ASCs were transfected with a lentiviral vector knocking down DUXAP10 (sh-DUXAP10) or a control vector (sh-NC). Subsequently, the cells were assessed using the following assays. (**D**) Statistical analyses of the data in **E**. (E) Representative fluorescent images of proliferative ASCs after transfection with the above vectors; the nuclei of all cells were labeled with Hoechst 33342, resulting in a blue fluorescence, while the actively proliferating cell nuclei were labeled with EdU, producing a green fluorescence; $n = 5$, scale bar = 50 μm. (**F**) Statistical analyses of the data in G. (**G**) Representative images of migratory ASCs after transfection with the above vectors; $n = 5$, scale bar = 100 μm. (**H**) Statistical analyses of the data in I. (**I**) Representative images of senescent ASCs after transfection with the above vectors; $n = 5$, scale bar = 50 μm. (**J**) Statistical analyses of the data in **K**. (K) Representative images of migratory fibroblasts treated with the conditioned media of ASCs after transfection with the above vectors; $n = 5$, scale bar = 200 μm. (**L**) Statistical analyses of the data in **M**. (M) Western blot analyses of the expression levels of FN1 and P21 in ASCs after DUXAP10 modification; $n = 3$. (**N**) PCR analyses of the expression levels of IL-6, IL-8, and TNF-α in ASCs after transfection with the above vectors; $n = 3$. *$P < .05$, **$P < .01$, ***$P < .001$, ****$P < .0001$.
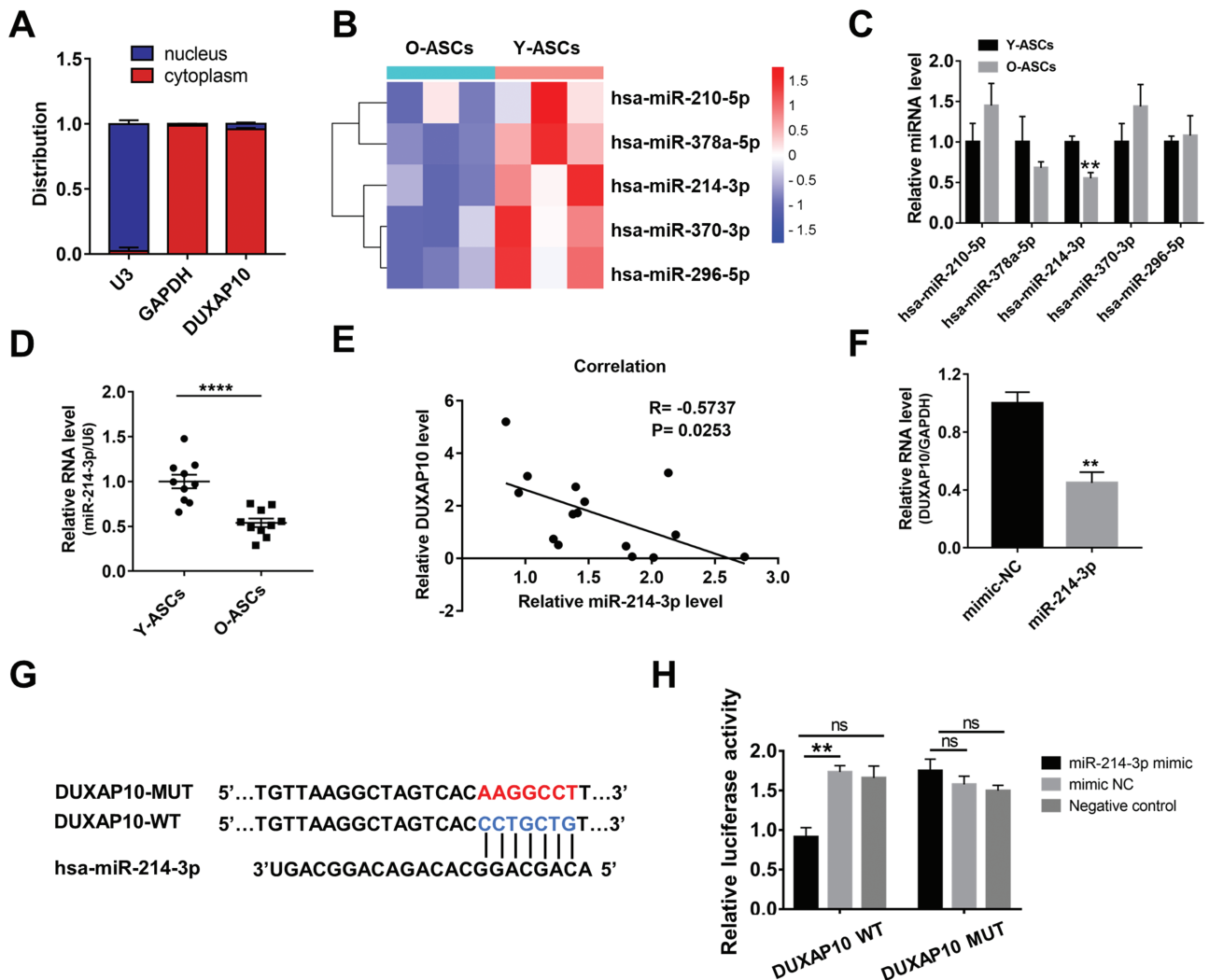
Figure 3. Cytoplasmic DUXAP10 functioned as a decoy for miR-214-3p. (**A**) PCR validation of the cellular location of DUXAP10. (**B**) Heatmap exhibiting 5 downregulated miRNAs in aged ASCs, which could also be sponged by DUXAP10. (**C**) PCR validation of the levels of those miRNAs; $n = 6$. (**D**) PCR validation of the level of miR-214-3p between O-ASC and Y-ASC; $n = 10$. (**E**) PCR analyses of the expressional correlation between DUXAP10 and miR-214-3p; $n = 15$. (**F**) PCR validation of the level of DUXAP10 after miR-214-3p overexpression in ASCs; $n = 3$. (**G**) The sequences of DUXAP10-WT and DUXAP10-MUT were inserted into the psi-CHECK-2 vector and prediction of binding sequences between DUXAP10 and miR-214-3p. (**H**) Luciferase activities of recombinant vectors with wildtype or mutated-type DUXAP10 was examined in HEK-293 T cells by co-transfection with miR-214-3p mimic and mimic NC; $n = 3$. *$P < .05$, **$P < .01$, ***$P < .001$, ****$P < .0001$.

miR-214-3p Improves Phenotypes in O-ASC and Enhances Stem Cell Function

Mimics and antagomirs were used to overexpress and knock-down miR-214-3p in ASC to detect ASC's function. EdU and transwell migration assays showed that miR-214-3p mimic augmented the proliferative and migrative abilities of O-ASC, while miR-214-3p antagomir impaired these abilities in Y-ASC (Fig. 4A-4D). Furthermore, transfection with miR-214-3p mimic resulted in a significant reduction in the rate of senescent cells in O-ASC, whereas the inhibition of miR-214-3p increased cell senescence in Y-ASC (Fig. 4E, 4F). Media conditioned by O-ASC transfected with miR-214-3p mimic exhibited superior fibroblast migration-promoting capacities than the negative control, while miR-214-3p antagomir noticeably damaged this function of conditional media isolated from Y-ASC (Fig. 4G, 4H). Additionally, miR-214-3p mimic's presence engineered an increase in FN1 expression and a decrease in p21 expression in aged ASCs; in contrast,

the inhibition of miR-214-3p in Y-ASC produced the opposite result (Fig. 4I, 4J). miR-214-3p mimic also promoted cyclin D1 expression and inhibited the secretion of senescence-associated factors, such as IL-6, MMP2, and TNF-α, in aged ASCs (Fig. 4K).

The Over-Expression of miR-214-3p Reverses the Adverse Effect of DUXAP10

To establish miR-214-3p's potential mediation in the function of DUXAP10, ASCs were co-transfected with miR-214-3p mimics and DUXAP10-overexpressed vectors. Co-transfection with miR-214-3p mimics remarkably reversed DUXAP10's inhibition of ASC proliferation and migration (Fig. 5A-5D). Meanwhile, the proportion of senescent cells and the fibroblast migration-promoting capacity of conditional media in co-transfected ASCs diminished and improved separately, compared to ASCs transfected with DUXAP10-overexpressed vectors alone (Fig. 5E-5H).
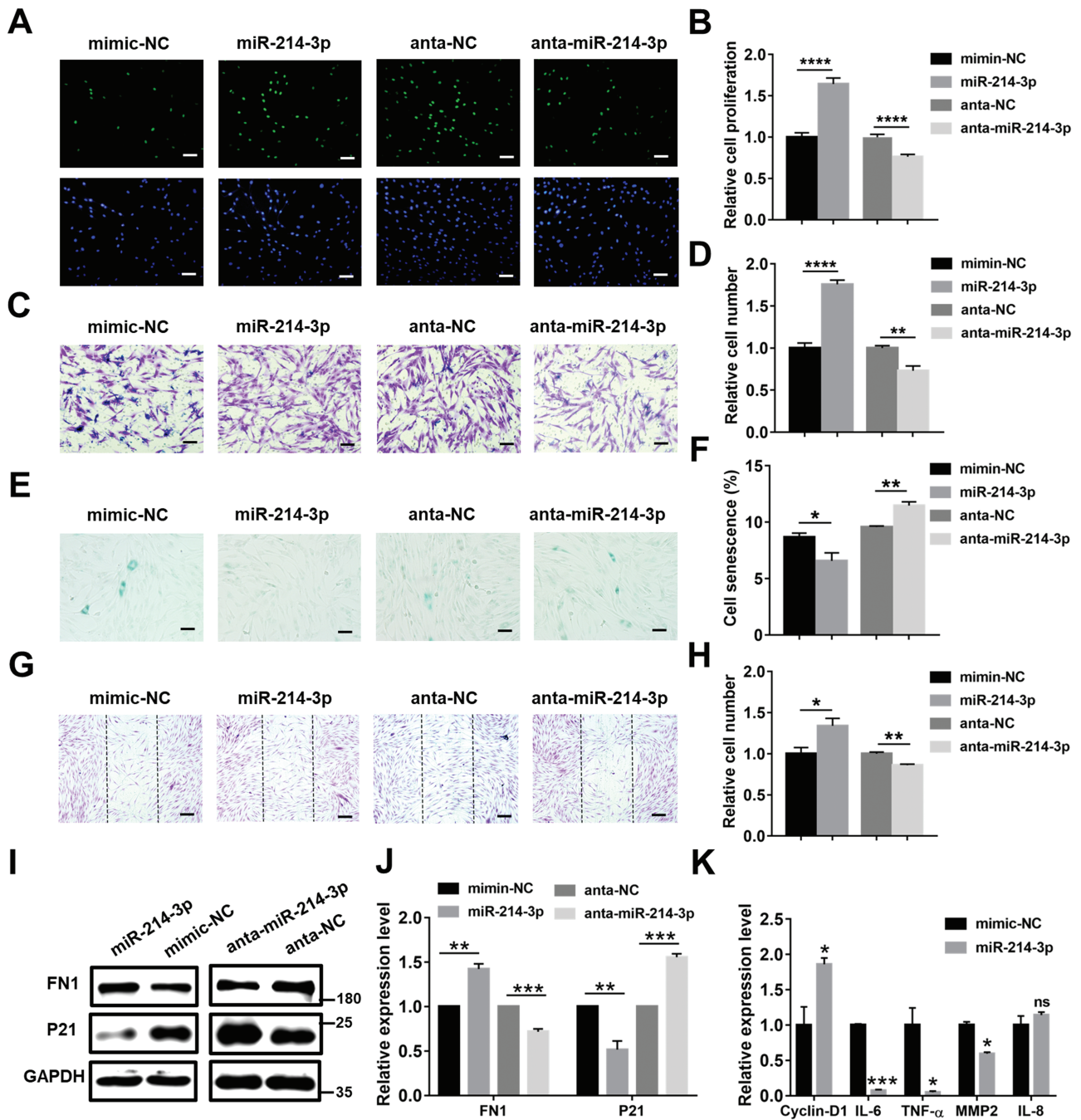
Figure 4. miR-214-3p overexpression rejuvenated aged ASCs, while its inhibition impaired young ASCs. Aged ASCs were given the miR-214-3p mimic or mimic NC through transfection, while young ASCs were transfected with the miR-214-3p inhibitor (anta-miR-214-3p) or a negative control (anta-NC). Subsequently, the cells were assessed using the following assays. (**A**) Representative fluorescent images of proliferative ASCs after transfection with the above oligonucleotides; *n* = 5, scale bar = 50 μm. (**C**) Images of migratory ASCs after transfection with the above oligonucleotides; *n* = 5, scale bar = 100 μm. (**E**) Representative images of senescent ASCs after transfection with the above oligonucleotides; *n* = 5, scale bar = 100 μm. (**G**) Images of migratory fibroblasts treated with the conditioned media of ASCs after transfection with the above oligonucleotides; *n* = 5, scale bar = 200 μm. (**B**, **D**, **F**, **H**) Statistical analyses of the data in A, C, E, and G. (**I**) Western blot analyses of the expression levels of FN1 and P21 in ASCs after transfection with the above oligonucleotides; *n* = 3. (**J**) Statistical analyses of the data in I. (**K**) PCR analyses of the expression levels of cyclin-D1, MMP2, IL-6, IL-8, and TNF-α in ASCs after transfection with the above oligonucleotides; *n* = 3. *$P < .05$, **$P < .01$, ***$P < .001$, ****$P < .0001$.

Furthermore, the co-transfection of ASCs with miR-214-3p mimics notably rescued the decline in FN1 and the rise in p21 induced by DUXAP10 overexpression (Fig. 5I, 5J), with the expression levels of DUXAP10 proportionally reduced by miR-214-3p mimics treatment in DUXAP10-overexpressed ASCs (Fig. 5K).

RASSF5 is a Potential Target of miR-214-3p in the Execution of Beneficial Functions

To identify the downstream effector of miR-214-3p, the bioinformatics databases listed above were used to predict potentially targeted mRNAs. Combining these mRNAs with mRNAs downregulated in Y-ASC, according to the
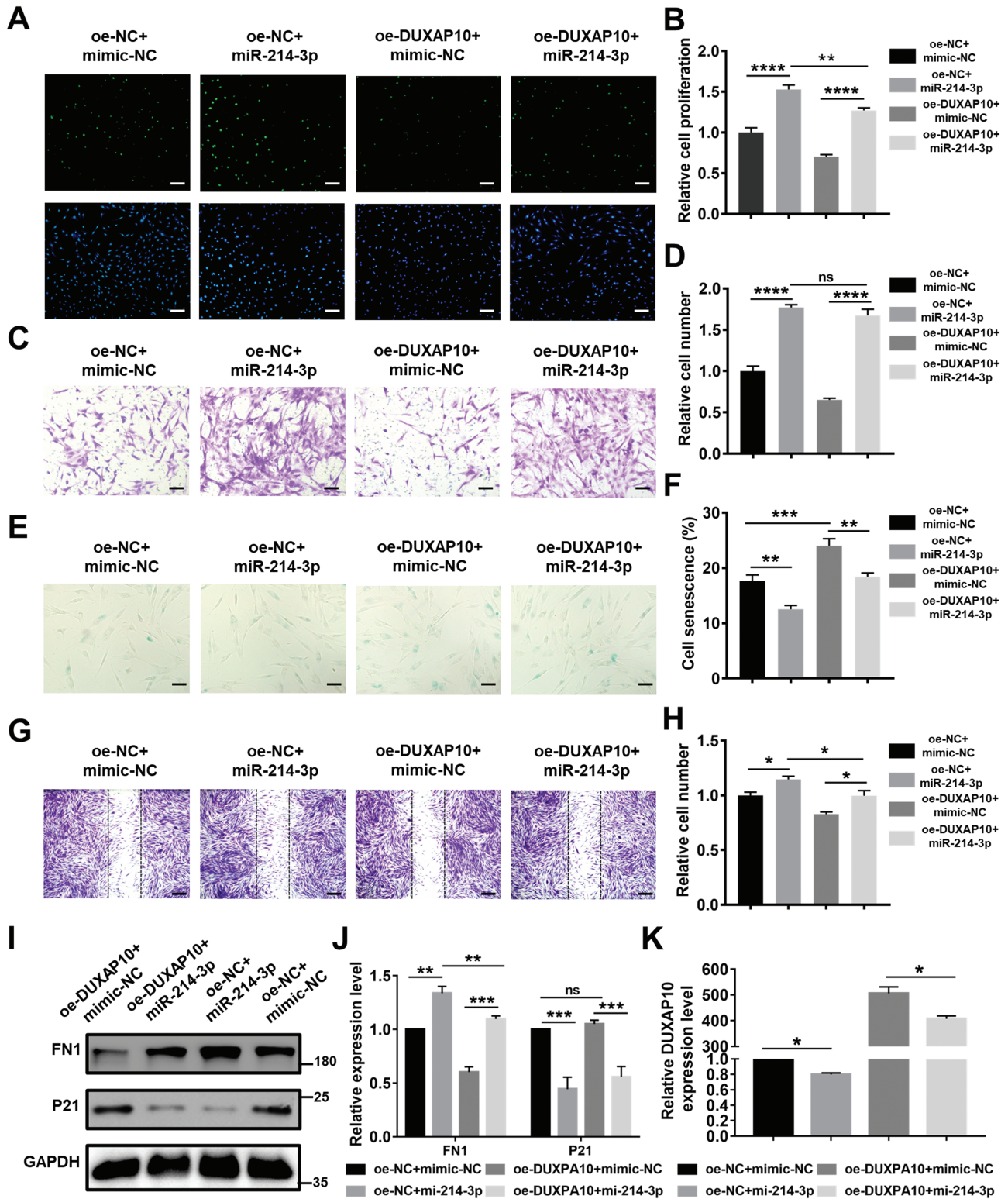
Figure 5. DUXAP10 overexpression reduced the beneficial effects of miR-214-3p. (**A**) Representative fluorescent images of proliferative ASCs after co-transfection with the miR-214-3p mimic and DUXAP10 overexpressed lentiviral vector; *n* = 5, scale bar = 100 µm. (**C**) Images of migratory ASCs after co-transfection; *n* = 5, scale bar = 100 µm. (**E**) Representative images of senescent ASCs after co-transfection; *n* = 5, scale bar = 50 µm. (**G**) Images of migratory fibroblasts treated with the conditioned media of ASCs after co-transfection; *n* = 5, scale bar = 200 µm. (**B**, **D**, **F**, **H**) Statistical analyses of data in (A, C, E, G). (**I**) Western blot analyses of the expression levels of FN1 and P21 in ASCs after co-transfection; *n* = 3. (**J**) Statistical analyses of the data in I. (**K**) PCR analyses of the expression levels of DUXAP10 in ASCs after co-transfection; *n* = 3. *$P < .05$, **$P < .01$, ***$P < .001$, ****$P < .0001$.
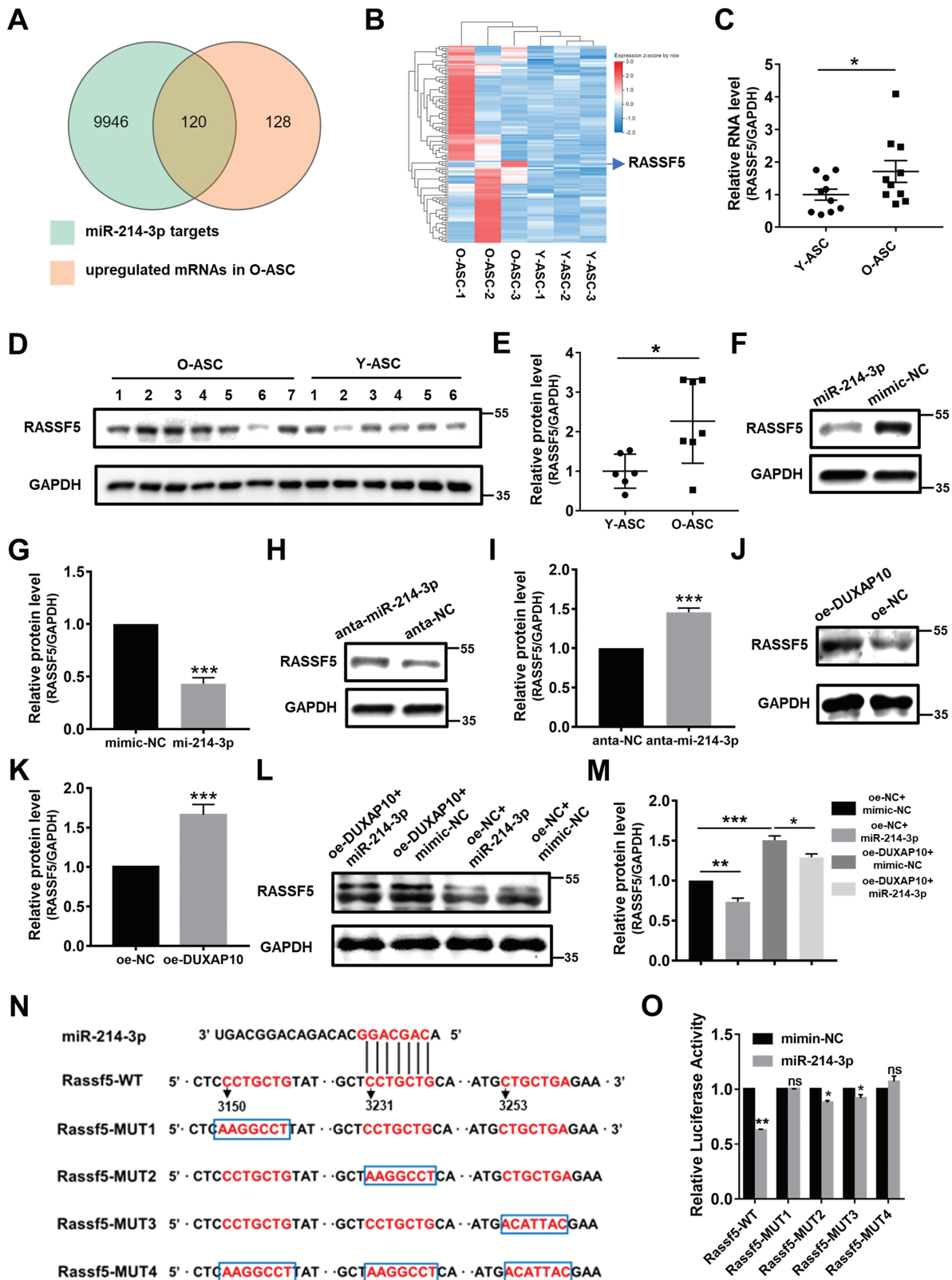
Figure 6. RASSF5 was the target of miR-214-3p. (**A**) Overlap of predicted miR-214-3p targets and genes upregulated in aged ASCs. (**B**) Heatmap exhibiting overlapped genes. (**C**) PCR validation of the expression level of RASSF5 between O-ASC and Y-ASC; *n* = 10. (**D**) Western blot analyses of the expression level of RASSF5 between O-ASC and Y-ASC. (**E**) Statistical analyses of the data in D. (**F**) Western blot analyses of the expression level of RASSF5 in aged ASCs after transfection with the miR-214-3p mimic or mimic NC; *n* = 3. (**G**) Statistical analyses of the data in F. (**H**) Western blot analyses of the expression level of RASSF5 in young ASCs after transfection with the anta-miR-214-3p or anta-NC; *n* = 3. (**I**) Statistical analyses of the data in H. (**J**) Western blot analyses of the expression level of RASSF5 in young ASCs after transfection with the oe-DUXAP10 or oe-NC vectors; *n* = 3. (**K**) Statistical analyses of the data in J. (**L**) Western blot analyses of the expression level of RASSF5 in ASCs after co-transfection with the miR-214-3p mimic and DUXAP10 overexpressed lentiviral vector; *n* = 3. (**M**) Statistical analyses of the data in L. (**N**) The sequences of RASSF5-WT and RASSF5-MUTs were inserted into the psi-CHECK-2 vector and prediction of binding sequences between RASSF5 and miR-214-3p. (**O**) Luciferase activities of recombinant vectors with wildtype or mutated-type RASSF5 was examined in HEK-293 T cells by co-transfection with the miR-214-3p mimic and mimic NC; *n* = 3. *$P < .05$, **$P < .01$, ***$P < .001$.

previous RNA-seq data, 120 candidate genes, which have been illustrated and clustered in Fig. 6A, 6B, were obtained. The GO database was then used to characterize the biological functions of these genes. RASSF5 (Ras Association Domain Family Member 5), a member of the Ras association domain family, was found to be associated with cell senescence, thus, arousing our interest. PCR analyses revealed that the expression levels of RASSF5 were upregulated significantly in O-ASC compared to Y-ASC (Fig. 6C). The Western blot analysis also showed much higher RASSF5 protein levels in O-ASC than in Y-ASC (Fig. 6D, 6E). Moreover, the over-expression of miR-214-3p reduced RASSF5 protein levels in ASC, while its inhibition promoted cellular RASSF5 expression (Fig. 6F-6I). On the other hand, the overexpression of DUXAP10 promoted RASSF5 expression (Fig. 6J, 6K) and rescued the miR-214-3p mimics treatment-caused decrease in RASSF5 (Fig. 6L, 6M). Bioinformatic analyses found 3 potential miR-214-3p binding sites in the RASSF5 transcript. Five psicheck2 plasmids containing wild and mutant 3′UTR sequences of the RASSF5 transcript were subsequently constructed, as shown in Fig. 6N. Per the dual-luciferase reporter assay, miR-214-3p bound to all these sites: the first site starting at the nucleotide position 3150nt displayed the highest affinity (Fig. 6O), suggesting that miR-214-3p binds directly to the RASSF5 transcript. Additionally, ASCs were co-transfected with si-RASSF5 and DUXAP10-overexpressed vectors to investigate their regulatory relationship. The efficiency of siRNAs targeting RASSF5 was assessed using the PCR and Western blot analyses (Supplementary Fig. S2A-S2C). Accordingly, co-transfection with si-RASSF5 reversed DUXAP10-overexpressed vectors' inhibition of ASC proliferation and migration (Supplementary Fig. S2D-S2G), as well as DUXAP10-overexpressed vectors' ability to stimulate ASC senescence (Supplementary Fig. S2H-S2I). Furthermore, the co-transfection of ASCs with si-RASSF5 notably rescued the decline in cyclin-D1 and the rise in IL-6 and IL-8 induced by DUXAP10 overexpression (Supplementary Fig. S2J-S2L).

DUXAP10 Knockdown Enhances the Therapeutic Ability of O-ASC to Heal Skin Wounds

To further assess DUXAP10 knockdown's potential to augment the beneficial effect of O-ASC on human diseases, O-ASC was transplanted into cutaneous wound beds on rats. According to our results, rats treated with sh-DUXAP10 O-ASC harbored significantly smaller unhealed wound areas than rats subjected to sh-NC O-ASC and PBS controls on days 12 and 15 post-transplantation (Fig. 7A-7C). Meanwhile, skin wounds transplanted with Y-ASC healed the fastest. HE staining assay also showed considerably narrower wound edge lengths in the sh-DUXAP10 O-ASC group than in the other 2 control groups, but these wound edge lengths were compatible with those in the sh-NC Y-ASC group (Fig. 7D, 7E). Per findings with the Masson staining assay, the sh-DUXAP10 O-ASC treatment drastically promoted collagen deposition in wound beds (Supplementary Fig. S3A, S3B). The IHC staining of PCNA revealed a substantially higher rate of proliferative cells in the sh-DUXAP10 O-ASC group than in the other 2 control groups but a lesser rate than in the sh-NC Y-ASC group (Supplementary Fig. S3C, S3D). Immunofluorescent staining of α-SMA showed that wound beds transplanted with sh-DUXAP10 O-ASC and sh-NC

Y-ASC had more abundant vessels than beds transplanted with sh-NC O-ASC and PBS (Supplementary Fig. S3E, S3F). Furthermore, the examination of frozen skin sections using fluorescent analysis revealed the existence of ASCs in the wound sites of all experimental groups that underwent cell transplantation (Supplementary Fig. S4). In conclusion, O-ASC accelerates skin wound healing by promoting cellular proliferation, neovascularization and collagen deposition in vivo, and DUXAP10 knockdown in O-ASC radically augments these benefits, which are comparable to Y-ASC.

Discussion

Stem cell aging is becoming a huge obstacle for ASC-based therapy. Understanding the mechanisms of age-related ASC dysfunction should provide opportunities to rejuvenate and energize these aging cells for clinical application. In the present study, DUXAP10 was found to be a positive regulator of ASC senescence and disability induced by aging. DUXAP10 was also revealed to impair the phenotype and function of ASCs by acting as a miR-214-3p sponge for promoting RASSF5 expression.

Recent studies have proven that lncRNAs participate in stemness maintenance and in multiple pathways regulating the aging process.[16] However, the overwhelming majority of these lncRNAs remain unannotated, highlighting a huge unexploited island for stem cell empowerment. Several lncRNAs have been shown to be dysregulated in aged stem cells and represent potential targets for stem cell rejuvenation. LncRNA NEAT1[21] and Bmncr[18] are up- and downregulated in aged BMSCs separately, and modulating their levels reverses the aged-related BMSC switch between adipocyte and osteoblast differentiation. Likewise, lnc-CYP7A1-1 has been found to be significantly increased in aged human BMSCs, and downregulating this lncRNA decreases cell senescence and increases cell proliferation and migration.[22] The expression of lncRNA HOTAIR is highly increased in renal stem/progenitor cells, and the knockout of HOTAIR leads to the senescence of these cells.[23] These earlier studies show that the modulation of lncRNAs could restore aged stem cell function. The present study established that lncRNA DUXAP10 originating from the pseudogene markedly accumulates in aged ASCs, and its silencing attenuates aged cell senescence and the secretion of proinflammatory cytokines (IL-8, TNF-α) but enhances cell proliferation, migration, and the therapeutic capacity for wound repair. Unlike the negative function in ASCs, DUXAP10 has been well-documented to exert oncogenic properties in various carcinomas and promote the proliferation of gastric, pancreatic, prostate, and osteogenic cancer cells.[19,24-26] This discrepancy possibly stems from the high tissue and cell type specificity of lncRNAs.

The biological functions of lncRNAs are diverse, depending on their location and specific interactions with proteins, RNA, and DNA.[15] In nuclei, lncRNAs can regulate chromatin remodeling and the transcription of neighboring and distant genes. LYPLAL1-AS1, a lncRNA located on the ASC nucleus, can bind the promoter of MIRLET7B and regulate its transcription.[17] DUXAP10, mainly located on the gastric cancer cell nucleus, can interact with PRC2 and LSD1 to repress LATS1 expression at the transcriptional level.[19] DUXAP10 is also located on the esophageal squamous cancer cell nucleus and epigenetically silences p21 expression by binding with EZH2.[27] In the present study, more than 95% of DUXAP10
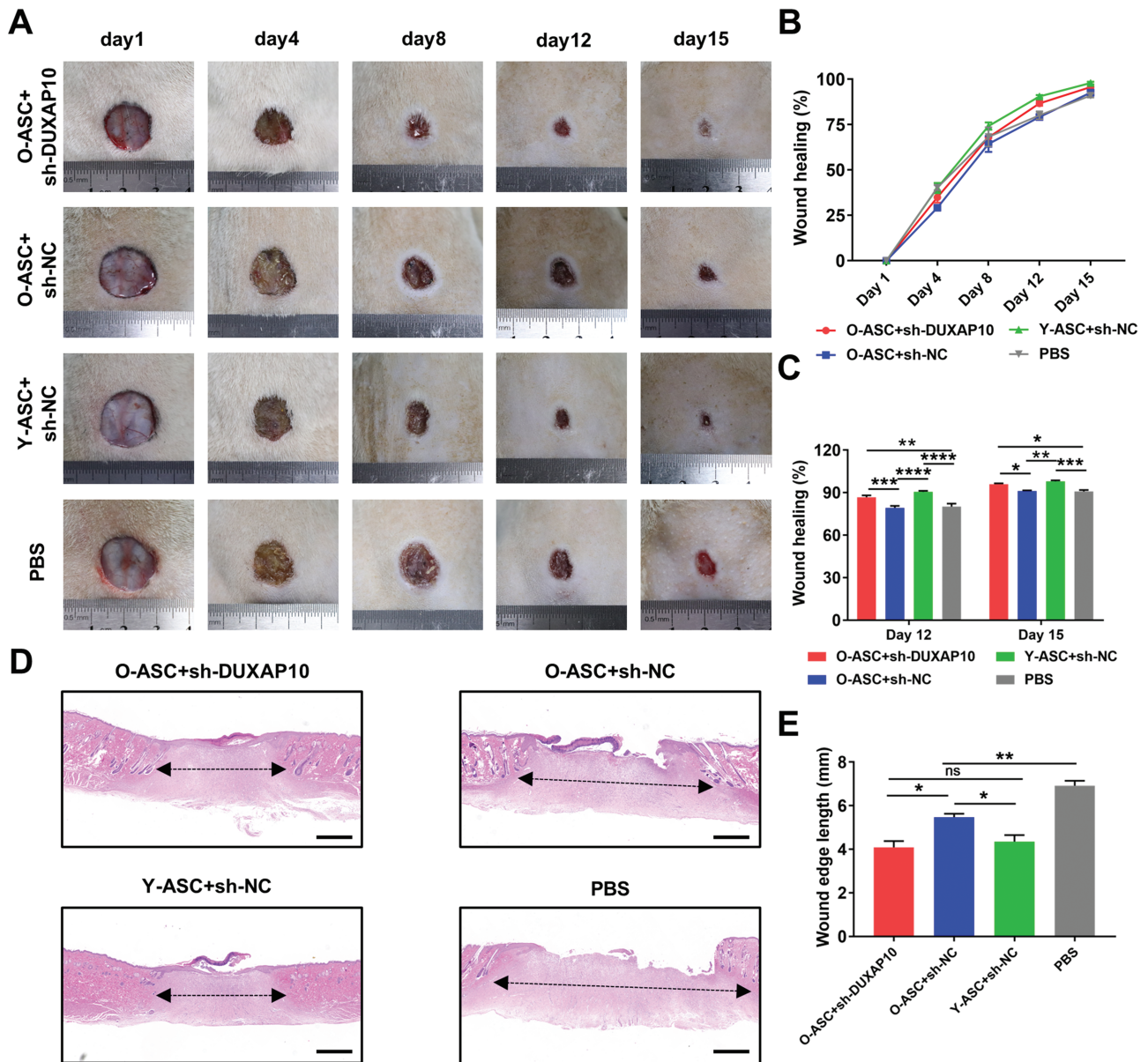
Figure 7. Knocking down DUXAP10 enhanced the therapeutic ability of aged ASCs for wound healing. (**A**) Representative images of skin wounds at days 1, 4, 8, 12, and 15. (**B**) Quantitative analyses of the wound-closure rates in different treatment groups. (**C**) Statistical analyses of the wound-closure rates in different treatment groups at day 12 and 15. (**D**) H&E staining analyses of wound sections at day 15; the double-headed arrows represent edges of the granulation; scale bar: 1 mm. (**E**) Quantitative analyses of the wound edge length in different treatment groups. N = 5. *P < .05, **P < .01, ***P < .001, ****P < .0001.

was found on the cytoplasm. Cytoplastic lncRNAs can sponge miRNAs, pair with other RNAs to recruit protein complexes, or directly interact with proteins. Previous studies have shown that DUXAP10 located in the nuclei of cancer cells recruit HuR to increase the stability of Sox12[28] and Sox18[26] mRNAs or sponge microRNA-1914.[29] LncRNA ENST00000563492 functions as a ceRNA for miR-205-5p to promote the osteogenesis of BMSCs.[30] First, DUXAP10's ability to function as a miRNA decoy was assessed since many miRNAs have been found to be dysregulated in aged ASCs. Bioinformatic analyses and PCP validation combinedly showed that miR-214-3p is a special target for sponging by DUXAP10. The expression correlation and specific binding sites between DUXAP10 and miR-214-3p were established using PCR and the dual-luciferase reporter assays. The

increased expression of miR-214-3p resulted in a decrease in the levels of DUXAP10 and mitigated the detrimental effects caused by DUXAP10 in aged ASCs. Conversely, elevating the levels of DUXAP10 did not result in a decrease in miR-214-3p levels. This suggests a potential mechanism where miR-214-3p may degrade DUXAP10 through potential interaction with the AGO2 protein. On the other hand, DUXAP10 seems to sequester miR-214-3p from other targets, such as RASSF5, rather than causing degradation of the microRNA. The diminished expression of miR-214-3p in aged ASCs may be regulated by alternative mechanisms. Nevertheless, other functions of cytoplasmic DUXAP10 in ASCs, such as a scaffold for RNAs and proteins, should be scrutinized further.

Various miRNAs have been reported to be involved in the age-related dysfunction of tissue stem cells.[31] miR-153

is downregulated in the hippocampi of aged mice, and its overexpression improves the neurogenesis of neural stem cells.[32] The expression of miR-155-5p[33] and miR-141-3p[34] in BMSC increases with age, and downregulating miR-155-5p rejuvenates aged BMSC and enhances their abilities for cardiac protection following infarction. Recent studies have revealed that miR-483-3p[35] and miR-34a[36] are significantly upregulated in ASCs during in vitro passaging, and inhibiting them reduces cellular senescence. However, the fundamental roles of miRNAs in the loss of ASCs' function during aging remain largely unknown. In this present investigation, miR-214-3p, as a target of DUXAP10, was visibly downregulated in aged ASCs. The increased expression of miR-214-3p significantly boosted the proliferation of aged ASCs and reduced cell senescence. However, the positive effects of miR-214-3p were partially counteracted by the overexpression of DUXAP10. Moreover, our results suggest that altering miR-214-3p had a more substantial impact on aged ASCs compared to modifying DUXAP10. This difference may be due to the ease of delivering miRNAs, as demonstrated by the significant upregulation of miR-214-3p by over a thousand-fold post-transfection with the miR-214-3p mimic. Additionally, lentiviral transfection-mediated RNA modification may pose risks to stem cells, complicating the evaluation of the relative significance and contribution of DUXAP10 and miR-214-3p to aged stem cells. Future research efforts should prioritize the development of more effective and secure approaches for RNA delivery. In the past, studies have paid more attention to the function of miR-214-3p modulating stem cell differentiation.[37,38] The current study highlights another function of miR-214-3p in rejuvenating aged stem cells, putting forward a potential target for the functional recovery of aged ASCs.

Most miRNAs are located on the cytoplasm and regulate gene expression post-transcriptionally. Earlier investigations uncovered various gene targets of miR-214-3p, including β-catenin[37] and BMP2[39] for osteogenic differentiation of BMSCs. The present study identifies RASSF5 as a specific target of miR-214-3p, with the expression of RASSF5 significantly elevated in aged ASCs. DUXAP10 overexpression or miR-214-3p inhibition both promoted RASSF5 expression. Importantly, there are 3 sites in the 3′UTR of RASSF5 for miR-214-3p binding, pointing to their strong interaction abilities. One past study examining one binding site between miR-214-3p and RASSF5 found that the overexpression of RASSF5 promoted oral cancer KB cell apoptosis.[40] RASSF5, also termed novel Ras effector 1A (NORE1A), is identified as a tumor suppressor and inactivated in many human cancers. Despite modulating apoptosis, RASSF5 is a powerful effector in Ras-induced cell senescence.[41] RASSF5 can scaffold both HIPK2 and PP1A to p53 and Rb in Ras-mediated senescence, and its overexpression induces cell senescence and decreases Ras-mediated transformation.[42] In the present study, knocking down RASSF5 reversed the harmful effect of DUXAP10 in ASCs, showing that RASSF5 and DUXAP10 accumulations are strongly associated with the poor function of stem cells during aging. Further studies must be conducted to explore the role and underlying mechanisms of RASSF5 in stem cell dysfunction with aging.

Adipose stem cells have been extensively studied for their potential in skin wound healing, particularly in the context of non-healing and chronic wounds associated with various conditions such as burns, pressure injuries, and diabetes mellitus.[43,44] However, the regenerative capabilities of these cells diminish with donor aging, diabetes, and prolonged in vitro culture, thereby limiting their clinical utility.[45] Previous research has explored several strategies to enhance the wound healing properties of ASCs, including the upregulation of miR-1248[46] or an anti-aging gene β-Klotho,[47] cultivation in a 3D coculture system,[48] and pre-treatment with a NOX1/4 inhibitor GKT137831[49] to mitigate reactive oxygen species production. In the current investigation, we have identified a novel approach wherein the knockdown of DUXAP10 enhances the therapeutic potential of aged ASCs in skin wound healing, as evidenced by improved wound collagen deposition, neovascularization, and accelerated wound closure. However, the functional enhancement of aged ASCs following DUXAP10 knockdown observed in in vitro experiments was not as pronounced in an acute skin wound model, likely due to the rapid healing nature of the model, which poses challenges in assessing treatment efficacy. Future studies should consider employing a chronic wound model, such as a diabetic wound model, to further elucidate the impact of DUXAP10 modification on the regenerative capacity of aged stem cells.

Conclusions

The present study demonstrated that DUXAP10 accumulation with aging contributes to the inferior phenotype and function of ASCs isolated from old donors. The underlying mechanism is the function of DUXAP10 as a decoy for miR-214-3p to enhance RASSF5 expression. Knocking down DUXAP10 and overexpressing miR-214-3p both promote aged ASC migration and proliferation but decreases cell senescence. Furthermore, DUXAP10 silencing enhances aged ASCs' therapeutic abilities to heal skin wounds. Overall, this study identifies an aged-related regulatory DUXAP10/miR-214-3p/RASSF5 axis, uncovering potential targets for rejuvenating and empowering dysfunctional adipose stem cells from old donors.

Acknowledgments

Funding

Conflict of Interest

The authors declared no potential conflicts of interest.

Author Contributions

S.R.: conceptualization; S.R., C.L., and H.X.: investigation. S.R., Z.X., B.S., L.D., and W.W.: methodology; Q.W. and X.W.: formal analysis. S.R.: funding acquisition. W.W. and X.L.: project administration. S.R.: original draft. J.C., X.L., and C.M.: writing and review and editing. All the authors read and approved the final manuscript.

Ethics Approval

Animal experiments were carried out in accordance with the guidelines and standards of the Experimental Animal Center of Tongji Medical College, Huazhong University of Science and Technology.

Consent to Participate

The use of samples from patients was conducted according to the guidelines of the Declaration of Helsinki and approved by the Ethics Committee of Tongji Medical College, Huazhong University of Science and Technology (No. 2022-S220). All the young donors' parents and adult donors have been informed in advance and consented to participate in this study.

Data Availability

The dataset generated and/or analyzed during the current study are available from the corresponding author on reasonable request.

Supplementary Material

Supplementary material is available at *Stem Cells Translational Medicine* online.

References

1. Oh J, Lee YD, Wagers AJ. Stem cell aging: mechanisms, regulators and therapeutic opportunities. *Nat Med*. 2014;20(8):870-880. https://doi.org/10.1038/nm.3651
2. Ermolaeva M, Neri F, Ori A, Rudolph KL. Cellular and epigenetic drivers of stem cell ageing. *Nat Rev Mol Cell Biol*. 2018;19(9):594-610. https://doi.org/10.1038/s41580-018-0020-3
3. Ren S, Chen J, Duscher D, et al. Microvesicles from human adipose stem cells promote wound healing by optimizing cellular functions via AKT and ERK signaling pathways. *Stem Cell Res Ther*. 2019;10(1):47-61.
4. Ren S, Chen J, Guo J, et al. Exosomes from adipose stem cells promote diabetic wound healing through the EHSP90/LRP1/AKT axis. *Cells* 2022;11(20):3229. https://doi.org/10.3390/cells11203229
5. Chen J, Ren S, Duscher D, et al. Exosomes from human adipose-derived stem cells promote sciatic nerve regeneration via optimizing Schwann cell function. *J Cell Physiol*. 2019;234(12):23097-23110.
6. Bacakova L, Zarubova J, Travnickova M, et al. Stem cells: their source, potency and use in regenerative therapies with focus on adipose-derived stem cells—a review. *Biotechnol Adv*. 2018;36(4):1111-1126. https://doi.org/10.1016/j.biotechadv.2018.03.011
7. Wang B, Liu Z, Chen VP, et al. Transplanting cells from old but not young donors causes physical dysfunction in older recipients. *Aging Cell*. 2020;19(3):13106-13109.
8. Ren S, Xiong H, Chen J, et al. The whole profiling and competing endogenous RNA network analyses of noncoding RNAs in adipose-derived stem cells from diabetic, old, and young patients. *Stem Cell Res Ther*. 2021;12(1):313-332.
9. Alicka M, Kornicka-Garbowska K, Kucharczyk K, et al. Age-dependent impairment of adipose-derived stem cells isolated from horses. *Stem Cell Res Ther*. 2020;11(1):4. https://doi.org/10.1186/s13287-019-1512-6
10. Kornicka K, Marycz K, Tomaszewski KA, et al. The effect of age on osteogenic and adipogenic differentiation potential of human adipose derived stromal stem cells (HASCS) and the impact of stress factors in the course of the differentiation process. *Oxid Med Cell Longev*. 2015;2015(1):1-20.
11. Zarychta-Wiśniewska W, Burdzińska A, Zielniok K, et al. The influence of cell source and donor age on the tenogenic potential and chemokine secretion of human mesenchymal stromal cells. *Stem Cells Int*. 2019;2019(1):1-14. https://doi.org/10.1155/2019/1613701
12. Brunet A, Goodell MA, Rando TA. Ageing and rejuvenation of tissue stem cells and their niches. *Nat Rev Mol Cell Biol*. 2023;24(1):45-62. https://doi.org/10.1038/s41580-022-00510-w
13. Borkowska J, Domaszewska-Szostek A, Kołodziej P, et al. Alterations in 5hmc level and genomic distribution in aging-related epigenetic drift in human adipose stem cells. *Epigenomics*. 2020;12(5):423-457.
14. Zhang H, Cai B, Geng A, et al. Base excision repair but not DNA double-strand break repair is impaired in aged human adipose-derived stem cells. *Aging Cell*. 2019;19(2):13062-13068.
15. Statello L, Guo CJ, Chen LL, Huarte M. Gene regulation by long non-coding RNAs and its biological functions. *Nat Rev Mol Cell Biol*. 2021;22(2):96-118. https://doi.org/10.1038/s41580-020-00315-9
16. Sousa-Franco A, Rebelo K, Da Rocha ST, Bernardes De Jesus B. LncRNAs regulating stemness in aging. *Aging Cell*. 2019;18(1):e12870. https://doi.org/10.1111/acel.12870
17. Yang Y, Liu S, He C, et al. LncRNA lyplal1-as1 rejuvenates human adipose-derived mesenchymal stem cell senescence via transcriptional mirlet7b inactivation. *Cell Biosci*. 2022;12(1):45-61.
18. Li C, Xiao Y, Yang M, et al. Long noncoding RNA Bmncr regulates mesenchymal stem cell fate during skeletal aging. *J Clin Invest*. 2018;128(12):5251-5266.
19. Xu Y, Yu X, Wei C, et al. Over-expression of oncigenic pesudogene DUXAP10 promotes cell proliferation and invasion by regulating lats1 and beta-catenin in gastric cancer. *J Exp Clin Cancer Res*. 2018;37(1):13. https://doi.org/10.1186/s13046-018-0684-8
20. Zhang W, Sun B, Zhao Y, et al. Proliferation of bovine myoblast by lncPRRX1 via regulation of the mir-137/CDC42 axis. *Int J Biol Macromol*. 2022;220(1):33-42. https://doi.org/10.1016/j.ijbiomac.2022.08.018
21. Zhang H, Xu R, Li B, et al. LncRNA neat1 controls the lineage fates of Bmscs during skeletal aging by impairing mitochondrial function and pluripotency maintenance. *Cell Death Differ*. 2022;29(2):351-365. https://doi.org/10.1038/s41418-021-00858-0
22. Dong J, Liu J, Wen Y, et al. Down-regulation of lnc-cyp7a1-1 rejuvenates aged human mesenchymal stem cells to improve their efficacy for heart repair through syne1. *Front Cell Dev Biol*. 2020;8(1):600304. https://doi.org/10.3389/fcell.2020.600304
23. Picerno A, Giannuzzi F, Curci C, et al. The long non-coding RNA hotair controls the self-renewal, cell senescence, and secretion of anti-aging protein alpha-klotho in human adult renal progenitor cells. *Stem Cells*. 2022;40(10):963-975. https://doi.org/10.1093/stmcls/sxac054
24. Lian Y, Xiao C, Yan C, et al. Knockdown of pseudogene derived from LncRNA duxap10 inhibits cell proliferation, migration, invasion, and promotes apoptosis in pancreatic cancer. *J Cell Biochem*. 2018;119(4):3671-3682. https://doi.org/10.1002/jcb.26578
25. Wang XF, Chen J, Gong YB, et al. Long non-coding RNA DUXAP10 promotes the proliferation, migration, and inhibits apoptosis of prostate cancer cells. *Eur Rev Med Pharmacol Sci*. 2019;23(9):3699-3708. https://doi.org/10.26355/eurrev_201905_17793
26. Wang G, Zhang Q, Wang Q, et al. Long non-coding RNA DUXAP10 exerts oncogenic properties in osteosarcoma by recruiting HuR to enhance SOX18 mRNA stability. *Hum Cell*. 2022;35(6):1939-1951. https://doi.org/10.1007/s13577-022-00772-8
27. Wang Z, Ren B, Huang J, et al. LncRNA duxap10 modulates cell proliferation in esophageal squamous cell carcinoma through epigenetically silencing p21. *Cancer Biol Ther*. 2018;19(11):998-1005. https://doi.org/10.1080/15384047.2018.1470723
28. Wu B, Yang C, Fang Y, Ding W, Zhang Y. Long noncoding RNA duxap10 promotes the stemness of glioma cells by recruiting HuR to enhance SOX12 mRNA stability. *Environ Toxicol*. 2021;36(5):840-849. https://doi.org/10.1002/tox.23087

29. Sun L, Wang L, Chen T, et al. Microrna-1914, which is regulated by LncRNA DUXAP10, inhibits cell proliferation by targeting the gpr39-mediated PI3K/AKT/mTOR pathway in HCC. *J Cell Mol Med*. 2019;23(12):8292-8304. https://doi.org/10.1111/jcmm.14705

30. Ouyang Z, Tan T, Zhang X, et al. LncRNA enst00000563492 promoting the osteogenesis-angiogenesis coupling process in bone mesenchymal stem cells (BMSCS) by functions as a ceRNA for mir-205-5p. *Cell Death Dis*. 2020;11(6):486. https://doi.org/10.1038/s41419-020-2689-4

31. Watanabe K, Ikuno Y, Kakeya Y, et al. Functional similarities of microRNAs across different types of tissue stem cells in aging. *Inflamm Regen*. 2018;38(1):9-13.

32. Qiao J, Zhao J, Chang S, et al. Microrna-153 improves the neurogenesis of neural stem cells and enhances the cognitive ability of aged mice through the notch signaling pathway. *Cell Death Differ*. 2020;27(2):808-825. https://doi.org/10.1038/s41418-019-0388-4

33. Hong Y, He H, Jiang G, et al. Mir-155-5p inhibition rejuvenates aged mesenchymal stem cells and enhances cardioprotection following infarction. *Aging Cell*. 2020;19(4):13128-13141.

34. Li Z, Ge X, Lu J, et al. Mir-141-3p regulates proliferation and senescence of stem cells from apical papilla by targeting yap. *Exp Cell Res*. 2019;383(2):111562. https://doi.org/10.1016/j.yexcr.2019.111562

35. Shen J, Zhu X, Liu H. Mir-483 induces senescence of human adipose-derived mesenchymal stem cells through igf1 inhibition. *Aging (Albany NY)* 2020;12(15):15756-15770. https://doi.org/10.18632/aging.103818

36. Mokhberian N, Bolandi Z, Eftekhary M, et al. Inhibition of mir-34a reduces cellular senescence in human adipose tissue-derived mesenchymal stem cells through the activation of sirt1. *Life Sci*. 2020;257(1):118055. https://doi.org/10.1016/j.lfs.2020.118055

37. Wang R, Zhang Y, Jin F, et al. High-glucose-induced mir-214-3p inhibits BMSCs osteogenic differentiation in type 1 diabetes mellitus. *Cell Death Discov*. 2019;5(1):143. https://doi.org/10.1038/s41420-019-0223-1

38. Jin F, Li M, Li X, et al. Dnmt1-mediated methylation inhibits microrna-214-3p and promotes hair follicle stem cell differentiate into adipogenic lineages. *Stem Cell Res Ther*. 2020;11(1):444. https://doi.org/10.1186/s13287-020-01864-8

39. Li J, Zhuang H, Wang Z, et al. LncRNAs malat1 and linc00657 upstream to mir-214-3p/bmp2 regulate osteogenic differentiation of human mesenchymal stem cells. *Mol Biol Rep*. 2022;49(7):6847-6857. https://doi.org/10.1007/s11033-022-07136-3

40. Li TK, Yin K, Chen Z, Bao Y, Zhang SX. Mir-214 regulates oral cancer kb cell apoptosis through targeting rassf5. *Genet Mol Res*. 2017;16(1):1-10. https://doi.org/10.4238/gmr16019327

41. Barnoud T, Schmidt ML, Donninger H, Clark GJ. The role of the nore1a tumor suppressor in oncogene-induced senescence. *Cancer Lett*. 2017;400(1):30-36. https://doi.org/10.1016/j.canlet.2017.04.030

42. Donninger H, Schmidt ML, Mezzanotte J, Barnoud T, Clark GJ. Ras signaling through RASSF proteins. *Semin Cell Dev Biol*. 2016;58(1):86-95. https://doi.org/10.1016/j.semcdb.2016.06.007

43. Brembilla NC, Vuagnat H, Boehncke WH, Krause KH, Preynat-Seauve O. Adipose-derived stromal cells for chronic wounds: scientific evidence and roadmap toward clinical practice. *Stem Cells Transl Med*. 2023;12(1):17-25. https://doi.org/10.1093/stcltm/szac081

44. Kohlhauser M, Tuca A, Kamolz LP. The efficacy of adipose-derived stem cells in burn injuries: a systematic review. *Cell Mol Biol Lett*. 2024;29(1):10. https://doi.org/10.1186/s11658-023-00526-w

45. Mazini L, Rochette L, Admou B, Amal S, Malka G. Hopes and limits of adipose-derived stem cells (ADSCS) and mesenchymal stem cells (MSCs) in wound healing. *Int J Mol Sci* . 2020;21(4):1306-1324.

46. Xiao S, Zhang D, Liu Z, et al. Diabetes-induced glucolipotoxicity impairs wound healing ability of adipose-derived stem cells-through the mir-1248/cited2/hif-1alpha pathway. *Aging (Albany Ny)* 2020;12(8):6947-6965. https://doi.org/10.18632/aging.103053

47. Laiva AL, O'Brien FJ, Keogh MB. Anti-aging beta-klotho gene-activated scaffold promotes rejuvenative wound healing response in human adipose-derived stem cells. *Pharmaceuticals*. 2021;14(11):1168-1183.

48. Hu W, Zhu S, Fanai ML, et al. 3d co-culture model of endothelial colony-forming cells (ECFCS) reverses late passage adipose-derived stem cell senescence for wound healing. *Stem Cell Res Ther*. 2020;11(1):355. https://doi.org/10.1186/s13287-020-01838-w

49. Dong Y, Zhang Y, Li F, et al. Gkt137831 in combination with adipose-derived stem cells alleviates high glucose-induced inflammaging and improves diabetic wound healing. *J Leukoc Biol*. 2023.